THE JOURNAL OF PHYSICAL CHEMISTRY C

Article

Cite This: J. Phys. Chem. C XXXX, XXX, XXX–XXX

pubs.acs.org/JPCC

Electronic Nature of Nonlinear Optical Properties of a Symmetrical Two-Photon Absorbing Fluorene Derivative: Experimental Study and Theoretical Modeling

Siarhei A. Kurhuzenkau,[†] Maria Yezabel Colon Gomez,[‡] Kevin D. Belfield,[§] Yevgeniy O. Shaydyuk,[∥] David J. Hagan,[#] Eric W. Van Stryland,[#] Cristina Sissa,[†] Mykhailo V. Bondar,[∥,*] and Anna Painelli[†,*]

[†]Department of Chemistry, University of Parma, Parco Area delle Scienze 17/A, Parma 43124, Italy

[‡]Department of Chemistry, University of Central Florida, Orlando, Florida 32816-2366, United States

[§]Department of Chemistry and Environmental Science, College of Science and Liberal Arts, New Jersey Institute of Technology, University Heights, Newark, New Jersey 07102, United States

[∥]Institute of Physics National Academy of Science of Ukraine, Prospect Nauki, 46, Kiev-28 03028, Ukraine

[#]CREOL, The College of Optics and Photonics, University of Central Florida, P.O. Box 162366, Orlando, Florida 32816, USA

Supporting Information

ABSTRACT: A comprehensive experimental and theoretical study of linear photophysical properties, such as excited-state relaxation, two-photon absorption, and stimulated emission spectra of the symmetrical fluorene derivative 2,2′-((1*E*,1′*E*)-(9,9-diethyl-9*H*-fluorene-2,7-diyl)bis(ethene-2,1-diyl))bis(1-methyl-1*H*-pyrrole) (**1**), is presented. The steady-state absorption, fluorescence, excitation, and excitation anisotropy spectra of **1** in organic solvents of different polarities are investigated experimentally and modeled. The fluorescence solvatochromism of **1** suggests the occurrence of symmetry breaking in the first excited state. The nature of fast relaxation processes in the excited state of **1**, with the characteristic times of several picoseconds, is investigated by transient absorption femtosecond pump−probe spectroscopy. The spectral properties of **1** are satisfactorily described by an essential-state model that, accounting for electron−vibration coupling and for polar solvation, addresses spectroscopic features not only in terms of band position and intensities but also in terms of band shapes. Specifically, we present the first calculation of frequency-resolved two-photon-excited fluorescence anisotropy spectra. Our results demonstrate that electron−vibration coupling and polar solvation quite naturally explain the puzzling experimental observation of large deviations of the anisotropies from the values expected on the basis of the relative orientation of the molecular transition dipole moments.

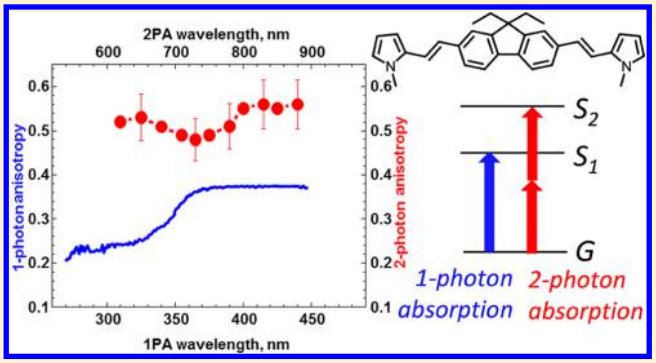

INTRODUCTION

Organic dyes have attracted much interest for several applications, including laser scanning fluorescence microscopy,[1,2] organic electronics,[3,4] nonlinear optics,[5,6] photodynamic therapy,[7,8] microfabrication, and high-density optical data storage.[9,10] Fluorene derivatives with specifically functionalized molecular structures[11−14] are promising candidates for two-photon absorption (2PA) applications. They exhibit strong vibronic interactions,[15,16] specific solvatochromic effects,[14,17] high fluorescence quantum yields,[18,19] photochemical stability,[20,21] large 2PA cross sections,[22,23] and stimulated emission efficiency.[15,24]

In this work, we present a comprehensive photophysical and photochemical study, supported by theoretical modeling, of a symmetrical fluorene derivative 2,2′-((1*E*,1′*E*)-(9,9-diethyl-9*H*-fluorene-2,7-diyl)bis(ethene-2,1-diyl))bis(1-methyl-1*H*-pyrrole) (**1**). The steady-state and time-resolved linear photophysical properties of **1**, including absorption, excitation, fluorescence, and one-photon excitation anisotropy spectra, lifetimes, and photodecomposition quantum yields, were investigated in solvents of different polarities. The two-photon excitation anisotropy spectrum was measured in a viscous medium, and the nature of its spectral shape was analyzed. Nonlinear optical characteristics, such as 2PA, excited-state absorption (ESA), and stimulated emission spectra of **1**, were obtained by two-photon-induced fluorescence, transient absorption pump−probe, and fluorescence quenching techniques, respectively, using a femtosecond laser system. Quantum mechanical analysis of the obtained experimental data was performed using the essential-state model (ESM) approach,

Received: December 18, 2017
Revised: February 16, 2018
Published: February 16, 2018

DOI: 10.1021/acs.jpcc.7b12397
J. Phys. Chem. C XXXX, XXX, XXX−XXX

rationalizing the symmetry breaking in the first excited electronic state of **1**, as well as 2PA and two-photon excitation anisotropy spectra.

EXPERIMENTAL SECTION

Synthetic Procedure for 1. The molecular structure of the new symmetrical fluorene derivative **1** is shown in Figure 1. A

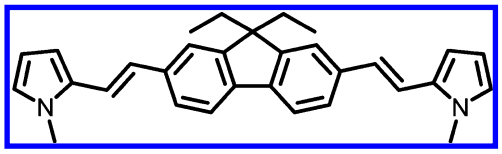

Figure 1. Chemical structure of **1**.

mixture of 2,7-bis(bromomethyl)-9,9-diethyl-9*H*-fluorene (1.5 g, 3.7 mmol) (prepared according to ref 25) and triethyl phosphite (5 mL) was refluxed for 2 h under N_2. Excess triethyl phosphite was distilled under reduced pressure. The residue was dried under vacuum and used directly for the subsequent Horner−Emmons reaction. The intermediate was dissolved in dry *N*,*N*-dimethylformamide (10 mL), followed by the slow addition of NaH (1.76 g, 73.3 mmol). The mixture was allowed to react under N_2 atmosphere at room temperature for **1**, followed by the addition of 1-methyl-1*H*-pyrrole-2-carbaldehyde (0.8 g, 7.3 mmol). The mixture was then stirred overnight at room temperature. Water was added, and the precipitate was collected by filtration, carefully washed with water, and dried. The crude product was purified by column chromatography with hexane/dichloromethane (DCM, 2:1) as an eluent. A yellow powder was obtained (1.09 g, 69%). mp 223−224 °C. ^{1}H NMR (500 MHz, $CDCl_3$): δ 7.62 (d, J = 7.9 Hz, 2H), 7.43 (d, J = 9.3 Hz, 2H), 7.37 (s, 2H), 7.01 (d, J = 16.2 Hz, 2H), 6.95 (d, J = 16.2 Hz, 2H), 6.64 (m, 2H), 6.50 (m, 2H), 6.17 (m, 2H), 3.73 (s, 6H), 2.07 (q, J = 7.3 Hz, 4H), 0.37 (t, J = 7.3 Hz, 6H). ^{13}C NMR (125 MHz, $CDCl_3$): δ 150.61, 140.56, 136.72, 132.28, 126.66, 125.01, 123.55, 120.32, 119.70, 116.30, 108.30, 106.67, 55.98, 34.23, 32.91, 8.61. HRMS (APCI) for $C_{31}H_{32}N_2$ theoretical m/z: $[M + H]^+$ 433.2638; found $[M + H]^+$, 433.2633.

Linear Photophysical and Photochemical Measurements. The steady-state absorption, fluorescence, excitation anisotropy, and lifetime measurements were performed in spectroscopic grade cyclohexane (CHX), toluene (TOL), tetrahydrofuran (THF), DCM, acetonitrile (ACN), and polyTHF (pTHF) at room temperature using a Lambda 650 (PerkinElmer) spectrophotometer and QuantaMaster (PTI, Inc.) and FluoroMax-3 (HORIBA Jobin Yvon) spectrofluorimeters. Fluorescence lifetimes of **1** were measured with a time-correlated single-photon counting system using 1 MHz laser excitation (excitation wavelength, $\lambda_{ex} \approx 403$ nm; pulse duration, $\tau_p \approx 250$ ps). The values of fluorescence quantum yields, Φ_{fl}, were determined following the procedure described in ref 26, using a fluorescein solution (0.1 M NaOH) as standard (Φ_{fl} = 0.92).[27] All fluorescence measurements were performed in dilute solutions (dye concentrations, $C \approx 10^{-6}$ M) and were corrected for the spectral response of the detection system. The quantum yields of the photochemical decomposition of **1** were obtained by the absorption methodology, as described in ref 20, using a continuous-wave Xe lamp irradiation ($\lambda_{ex} \approx 400$ nm; irradiation intensity, $I_0 \approx 5$ mW/cm^2).

2PA, Two-Photon Excitation Anisotropy, Stimulated Emission, and Transient Absorption Measurements. The degenerate 2PA spectrum of **1** was obtained by the two-photon-induced fluorescence method[28,29] (in combination with a PTI QuantaMaster spectrofluorimeter) using a 1 kHz femtosecond laser system (Ti:sapphire chirped-pulse-amplified Legend Duo+ Coherent, Inc., pumped optical parametric amplifier OPA HE-TOPAS Light Conversion, Inc., and after the second harmonic generation and using multiple 10 nm full width at half-maximum (fwhm) spike filters, we obtained pulse energy, $E_p \leq 10$ μJ and $\tau_p \approx 100$ fs over a broad spectral range). Experimental details may be found in ref 30. The same femtosecond laser beam input to a PTI QuantaMaster spectrofluorimeter was used for two-photon excitation anisotropy measurements, as comprehensively described in refs 31 and 32. The stimulated emission cross-sectional measurements were performed by the fluorescence quenching methodology.[15,33] In this case, the output beam of the Legend Duo+ regenerative amplifier at 800 nm was split in two parts. The first part was doubled by a 1 mm beta-borium borate (BBO) crystal and used as the fluorescence excitation beam at λ_{ex} = 400 nm, and the fluorescence signal was detected at a right angle to the incident beam with an HR4000 Ocean Optics spectrometer. The second beam at 800 nm pumped into an OPA TOPAS-800 fs (Coherent, Inc.) with a broad tuning range was used as the fluorescence-quenching beam. The transient absorption pump−probe setup was comprehensively described in refs 34 and 35. Briefly, the output of the Ti:sapphire regenerative amplifier, Legend F-1K-HE (Coherent, Inc.), at a wavelength of 800 nm, $E_p \approx 1$ mJ, $\tau_p \approx 140$ fs (fwhm), and a repetition rate of 1 kHz, was split into two parts. The frequency of the first beam was doubled by a 1 mm BBO crystal and used as the pump beam ($E_p \approx 5-10$ μJ). The second laser beam was focused into a sapphire plate to produce a white-light continuum and served as the probe beam ($E_p \leq 5$ nJ), delayed by an optical delay line, M-531.DD (PI, Inc.), relative to the pump beam. The pump and probe beams were overlapped at a small angle in the sample solution, and the probe transmittance was determined by an Acton SP500i spectrometer, equipped with a Spec 10 CCD detector. The angle between the linear polarizations of the pump and probe beams was set to 54.7°. The estimated time resolution of the employed technique was ≤300 fs. The sample solutions were placed in a 1 mm quartz flow cell to avoid possible thermo-optical effects and photochemical decomposition.

RESULTS AND DISCUSSION

Linear Photophysical and Photochemical Properties of 1. The steady-state linear absorption and fluorescence spectra, along with the main photophysical and photochemical parameters of **1**, are presented in Figure 2 and Table 1. The absorption spectra of **1** (Figure 2, curves 1−5) exhibited weak dependence on solvent polarity[26] and a partly resolved vibronic structure. No aggregation effects were observed up to $C \approx 10^{-2}$ M. The steady-state fluorescence spectra of **1** (Figure 2, curves 1′−5′) were independent of the excitation wavelength, and the excitation spectra perfectly matched the absorption bands, in agreement with Kasha's rule.[26] The absorption band was marginally affected by solvent polarity, while sizable solvatochromism was observed in emission, as expected for class I quadrupolar dye, exhibiting symmetry breaking in the first excited electronic state S_1.[36] The Stokes shift showed a linear dependence on solvent polarity (Figure S1) following the

DOI: 10.1021/acs.jpcc.7b12397
J. Phys. Chem. C XXXX, XXX, XXX−XXX

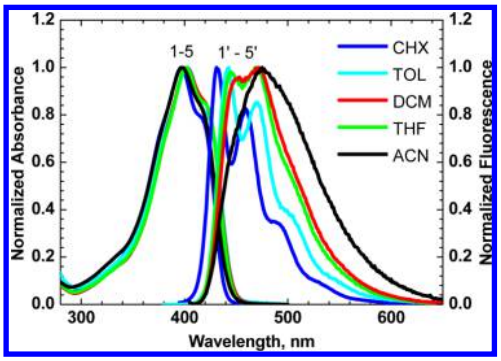

Figure 2. Normalized linear absorption (1−5) and fluorescence (1′−5′) spectra of **1** in CHX (1, 1′), TOL (2, 2′), THF (3, 3′), DCM (4, 4′), and ACN (5, 5′).

Lippert equation,[26] which demonstrates the absence of specific solute−solvent interactions,[37] in line with the almost constant values of maximum extinction coefficients ε^{max} in the investigated media (see data in Table 1).

Compound **1** was highly fluorescent and exhibited single-exponential fluorescence decay in all solvents, with the lifetimes slightly increasing with the solvent polarity. The natural lifetimes can be obtained from the fluorescence data, $\tau_n = \tau_{fl}/\Phi_{fl}$, and compared with the results obtained from the intensity of the linear absorption and fluorescence band, according to the Strickler−Berg equation[38]

$$1/\tau_n^{SB} = 2.88 \times 10^{-9} \times n^2 \times \frac{\int F(\nu)\, d\nu}{\int [F(\nu)/\nu^3]\, d\nu} \times \int [\varepsilon(\nu)/\nu]\, d\nu$$

where $F(\nu)$ and n are the fluorescence spectrum plotted in wavenumbers, cm^{-1}, and refractive index of the medium, respectively. The largest deviations between the two lifetime values were observed in more polar solvents where one expects the largest changes in the molecular configuration following electronic excitation.[39]

The fundamental anisotropy spectrum of **1** (Figure 3b, curve 1) was obtained for the highly viscous pTHF to ensure a much larger rotational correlation time than the fluorescence lifetime, $\theta_{rot} \gg \tau_{fl}$.[26] Under these conditions, according to the standard model, the value of fluorescence excitation anisotropy, r, is determined by the angle β between the absorption and emission transition dipole moments, $r = (3\cos^2\beta - 1)/5$.[26] The constant and large ($r > 0.35$) values of anisotropy in the

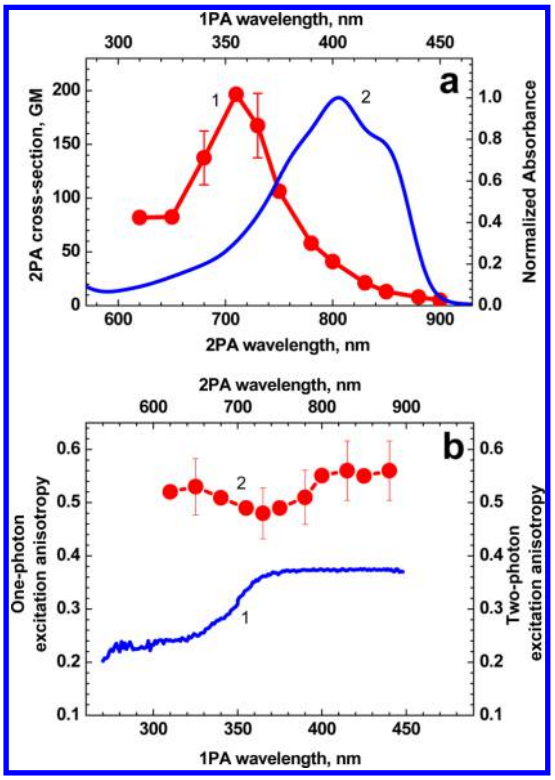

Figure 3. (a) Degenerate 2PA (1) and normalized linear absorption (2) spectra of **1** in TOL. (b) Two-photon excitation anisotropy (2) and steady-state one-photon excitation anisotropy (1) spectra of **1** in pTHF.

region of the main absorption band of **1** therefore suggest a single $S_0 \rightarrow S_1$ electronic transition (S_0 and S_1 are the ground and first excited electronic states, respectively). The anisotropy decreased to ~0.27 in the region of the $S_0 \rightarrow S_2$ transition (S_2 is the second excited electronic state), a slightly surprising result because for the symmetric bent quadrupolar dye the states can only be polarized either along the same direction as S_1 or perpendicular to it so that the only possible values of r_0 are 0.4 or −0.2. This discrepancy will be quantitatively addressed in the Theoretical Modeling section. In low-viscosity solvents where $\theta_{rot} \approx \tau_{fl}$, the values of anisotropy dramatically decreased because of rotational depolarization (Figure S2, curves 1−5).

The photochemical stability of **1** is studied in different solvents (for dye concentrations $C \approx 20-30\ \mu M$) using low-intensity excitation in the main long-wavelength absorption band, and the estimated photodecomposition quantum yields,

Table 1. Main Linear Photophysical and Photochemical Parameters of 1 in Solvents with Different Polarities: Absorption (λ_{ab}^{max}) and Fluorescence (λ_{fl}^{max}) Maxima; Maximum Extinction Coefficients ε^{max}; Fluorescence Quantum Yields Φ_{fl}; Experimental Fluorescence Lifetimes τ_{fl}; Natural Lifetimes $\tau_n = \tau_{fl}/\Phi_{fl}$; Natural Lifetimes from the Strickler−Berg Relation τ_n^{SB}; and Photodecomposition Quantum Yields Φ_{ph}

solvent	CHX	TOL	THF	DCM	ACN
λ_{ab}^{max}, nm	397	403	402	402	398
λ_{fl}^{max}, nm	431	442	471	472	474
ε^{max}, $M^{-1}\cdot cm^{-1}$	72 000	75 000	74 000	77 000	78 000
Φ_{fl}	0.62	0.70	0.60	0.50	0.52
τ_{fl}, ns	1.0	1.0	1.1	1.2	1.3
τ_n, ns	1.6	1.4	1.8	2.4	2.5
τ_n^{SB}, ns	1.4	1.4	1.6	1.5	1.8
Φ_{ph}	4×10^{-3}	5×10^{-3}	4×10^{-3}	5×10^{-3}	8×10^{-3}

DOI: 10.1021/acs.jpcc.7b12397
J. Phys. Chem. C XXXX, XXX, XXX−XXX

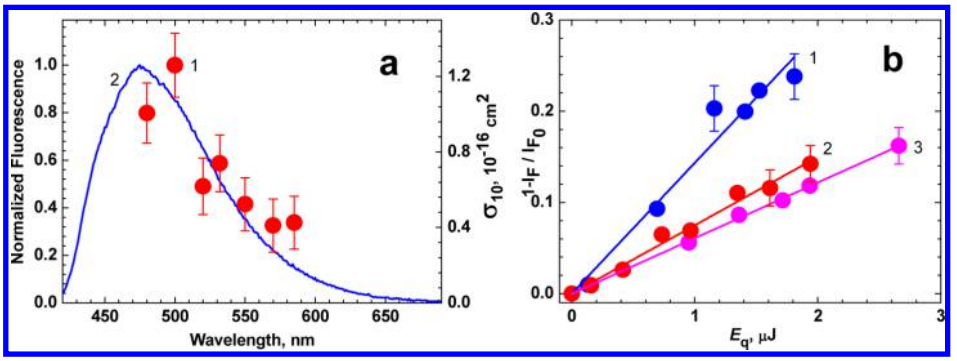

Figure 4. (a) Stimulated emission σ_{10} (1) and normalized fluorescence (2) spectra of **1** in ACN. (b) Experimental dependences $1 - I_F/I_{F_0} = f(E_q)$ for **1** in ACN: λ_q = 480 nm (1), 550 nm (2), and 580 nm (3).

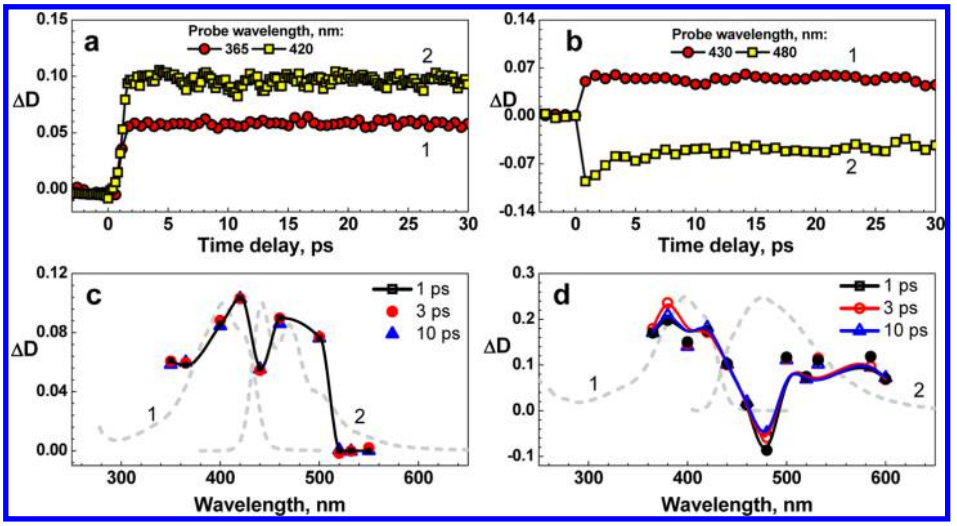

Figure 5. (a) Transient absorption kinetic dependences $\Delta D(\tau_D)$ for **1** in TOL for selected probing wavelengths: λ_p = 365 nm (1) and 420 nm (2); (b) transient absorption kinetic dependences $\Delta D(\tau_D)$ for **1** in ACN for λ_p = 430 nm (1) and 480 nm (2). (c) Time-resolved transient absorption spectra of **1** in TOL for τ_D = 1 ps (black squares), 3 ps (red circles), and 10 ps (blue triangles), and the steady-state linear absorption (1) and fluorescence (2) spectra of **1**. (d) Time-resolved transient absorption spectra of **1** in ACN for τ_D = 1 ps (black squares), 3 ps (red circles), and 10 ps (blue triangles), and the steady-state linear absorption (1) and fluorescence (2) spectra of **1**.

Φ_{ph}, are presented in Table 1. The estimated Φ_{ph} values are slightly larger than those for typical laser dyes,[40,41] but the combination of its high fluorescence quantum yield and 2PA cross section (see below) make fluorene **1** an interesting candidate for bioimaging applications.

2PA and Two-Photon Excitation Anisotropy of 1. The degenerate 2PA spectrum of **1**, obtained by the two-photon-induced fluorescence technique using rhodamine B in methanol and fluorescein in water (pH = 11) as standards,[29] is shown in Figure 3a. A single 2PA peak was observed with a maximum at 710 nm, with a cross-sectional value of ~200 GM. Indeed, for bent symmetric quadrupolar dyes, the S_1 state may also display 2PA activity;[19] however, the bending angle in **1** is too small to lead to a sizable 2PA intensity of S_1.

The anisotropy of fluorescence induced by 2PA processes, r_{2PA}, obtained for **1** in viscous pTHF is shown in Figure 3b. These data can be used to obtain information about the relative orientation of the transition dipole moments, including transition dipoles between the excited states, and can shed light on the nature of the excited states. According to the data in Figure 5, the fundamental values of r_{2PA} were very close to the theoretical maximum limit (r_{2PA}^{max} = 0.57),[26] exhibiting very weak dependence on the excitation wavelength over the entire spectral range studied at variance with the corresponding one-photon excitation anisotropy (Figure 3b, curve 1). A similar behavior was previously reported for polymethine and fluorene dyes in viscous solvents, and possible explanations for this phenomenon were discussed.[31,32] The nature of the dependence $r_{2PA}(\lambda_{exc})$ for the molecular structure of **1** is analyzed in the Theoretical Modeling section.

Stimulated Emission Spectra and Fast Relaxation Processes in 1. The stimulated emission cross section of organic molecules, σ_{10}, is of interest for applications in stimulated emission depletion (STED) microscopy,[42] superluminescence, and lasing.[6,43] Unfortunately, σ_{10} measurements are scarcely addressed in the literature. The values of $\sigma_{10}(\lambda)$ for **1** in ACN were determined by a fluorescence quenching method.[15] The results obtained in the fluorescence spectral range of 480−580 nm for fixed delay ~10 ps $\ll \tau_{fl}$ between the pump and quenching pulses are shown in Figure 4a. The degree of fluorescence quenching, $1 - I_F/I_{F_0}$ (where I_F and I_{F_0} are the integrated fluorescence intensities observed with and without the quenching beam with pulse energy E_q), is directly proportional to the product $\sigma_{10}(\lambda_q) \times E_q$, where λ_q is the quenching wavelength.[15] Typical nearly linear $1 - I_F/I_{F_0} = f(E_q)$ dependences measured in ACN at selected quenching wavelengths are shown in Figure 4b. The values of $\sigma_{10}(\lambda_q)$ were

DOI: 10.1021/acs.jpcc.7b12397
J. Phys. Chem. C XXXX, XXX, XXX−XXX

estimated from the slopes of the $f(E_q)$ curves. According to the data in Figure 4a, the stimulated emission spectrum is very similar to the fluorescence contour. The maximum value of $\sigma_{10} \approx 1.3 \times 10^{-16}$ cm^2 is significantly smaller than the corresponding maximum one-photon absorption cross section, $\sigma_{01} \approx 3 \times 10^{-16}$ cm^2, suggesting a slightly smaller transition dipole moment for the emission than for the absorption process, which is in line with the conclusions drawn from the comparison of the τ_n and τ_n^{SB} natural lifetimes (see Table 1).

The relaxation processes in **1** were investigated by a femtosecond transient absorption pump−probe technique[34] in nonpolar (TOL) and polar (ACN) aprotic solvents over a broad spectral range. The induced changes in the optical density, ΔD, were measured as a function of time delay, τ_D, between the probe and pump pulses and of the probe wavelength, λ_p, and are presented in Figure 5. The transient absorption kinetics of **1** revealed strong positive signals ($\Delta D > 0$) in the spectral range of the main absorption band (Figure 5a,c), suggesting the presence of efficient ESA processes that overwhelm the ground-state bleaching (i.e., saturable absorption). These ESA signals arise within the instrumental response time, remain nearly constant in the picosecond timescale, and then slowly relax to zero in accordance with the nanosecond fluorescence lifetime. This behavior suggests that all ultrafast dynamics subsequent to the electronic excitation, including vibrational relaxation processes, end within the first 300−500 fs after photoexcitation without any evidence of solvent reorganization dynamics in nonpolar TOL. In polar ACN, some evidence of optical gain ($\Delta D < 0$) was detected in the fluorescence spectral range (Figure 5b,d) of **1**, and the relaxation process with the characteristic time of ∼2−3 ps in the transient absorption signal at 480 nm is safely associated with the solvent reorientation around the excited chromophore.[14,19,24]

Theoretical Modeling. Low-energy linear and nonlinear optical spectra of charge-transfer organic dyes can be accurately described by ESMs, a family of semiempirical models that was developed and validated for different families of dyes[36,37,44−49] and aggregates.[50−52] The main concept behind ESM is to account for a reduced set of electronic basis states, the essential states, that correspond to the main resonating structures characteristic for each dye. For quadrupolar donor−acceptor−donor (DAD) dyes such as **1**, three basis (diabatic) electronic states are minimally needed, corresponding to the neutral state, $|N\rangle$ = DAD, and to the two zwitterionic states, $|Z_L\rangle = D^+A^-D$ and $|Z_R\rangle = DA^-D^+$. The two degenerate zwitterionic states are separated from the neutral state by an energy gap of 2η. The charge resonance is described by a mixing matrix element, $-\tau$, as described in the Supporting Information. The electronic Hamiltonian adopted for **1**, a bent quadrupolar dye, is exactly the same as discussed in ref 36, for linear quadrupolar dyes. However, the dipole moment operator must account for the bent nature of the dye, described by the angle α, measuring the deviation from linearity. As discussed in the Supporting Information, for linear dyes strict selection rules apply, with S_1 only active in 1PA and S_2 in 2PA. In bent molecules, both the states acquire intensity in both 1PA and 2PA, but for small bending angles, the selection rules for the linear dye are nearly maintained.

To properly address spectral band shapes, the coupling of electronic degrees of freedom to molecular vibrations must be accounted for. We introduce two effective coordinates, q_L and q_R, that describe the relaxation of the molecular geometry upon charge transfer along the two molecular arms. The two coordinates have the same frequency, ω_v, and relaxation energy, ε_v (see the Supporting Information for details). The coupled electron−vibrational Hamiltonian is written on the nonadiabatic basis generated as the direct product of the electronic basis times the eigenstates of the two harmonic oscillators related to q_L and q_R. Indeed, we truncate the vibrational basis to the maximum number M of states for each oscillator so that the basis has a dimension $3M^2$, ensuring to use large enough M so as to reach convergence. The diagonalization of the Hamiltonian matrix gives numerically exact vibronic eigenstates that enter the sum-over-state expressions for the calculation of optical spectra. An additional parameter, γ, enters the calculation, measuring the line width associated with each vibronic line.

Polar solvation is introduced in the model in the framework of the reaction field model. As discussed in refs 36 and 37, only the orientational component of the reaction field is explicitly discussed in ESMs. In the specific case of bent quadrupolar dyes, two components F_x and F_y of the reaction field are coupled to the dipole moment operator.[44] The solvation relaxation energy, ε_{or}, measuring the energy gained by a molecule upon relaxation along the solvation coordinate, is set to zero in nonpolar solvents and increases with the solvent polarity. In polar solvents, the electronic Hamiltonian becomes F_x and F_y-dependent (see the Supporting Information). The coupled electronic and vibrational Hamiltonian is therefore diagonalized numerically on a grid of F_x and F_y values, and relevant optical spectra are calculated as described in the Supporting Information at each point of the grid. The total spectra are finally obtained summing up the spectra calculated at each point of the grid, weighted according to the relevant Boltzmann distribution. Indeed, when dealing with absorption spectra, the Boltzmann distribution refers to the (F_x, F_y)-dependent energy of the ground state, whereas when dealing with fluorescence spectra, the Boltzmann distribution is calculated based on the energy of the fluorescent state. Along these lines, the model accounts not just for solvatochromism but also for the subtle effects of polar solvation on band shapes and specifically for inhomogeneous broadening effects. Finally, in the calculation of anisotropy spectra, both the distributions must be considered (see the Supporting Information for details).

Table 2 collects all molecular parameters entering the calculation of optical spectra, including absorbance, emission, 2PA, and linear and two-photon-induced fluorescence anisotropy. The model explicitly accounts for polar solvation, whereas the effect of the electronic degrees of freedom of the solvent is implicitly introduced via the dependence of model parameters on the solvent refractive index.[37] In view of the marginal variation of the refractive index in common organic solvents, all molecular parameters are kept fixed, and the spectroscopic effects of solvent polarity are accounted for adjusting a single parameter, ε_{or}, measuring the solvent relaxation energy.[37] We emphasize that band shapes are not adjusted by hand but are reproduced by the inhomogeneous

Table 2. ESM Parameters

η/eV	τ/eV	ε/eV	ω/eV	μ/debye	α/degrees	Γ/eV
1.42	0.8	0.48	0.18	29	20	0.08

DOI: 10.1021/acs.jpcc.7b12397
J. Phys. Chem. C XXXX, XXX, XXX−XXX

broadening and vibrational coupling effects that are included in the ESM.

The calculated absorption and emission spectra in Figure 6 agree very well with the experimental spectra in Figure 2. ESM

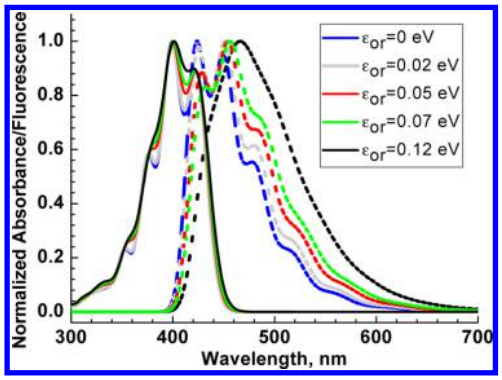

Figure 6. Normalized absorbance and fluorescence spectra (continuous and dashed lines, respectively) calculated by ESM with the molecular parameters in Table 2, and variation in ε_{or} to mimic the different polarities of the solvents in Figure 2. Specifically, blue, light blue, red, green, and black lines refer to the results obtained for ε_{or} = 0, 0.02, 0.05, 0.07, and 0.12 eV, respectively.

accurately reproduces the band shapes and positions of absorption and fluorescence spectra in solvents of different polarities, with the partially resolved vibronic structure observed in nonpolar solvents that blurs in polar solvents.

As for the 2PA spectra shown in Figure 7, we notice that the bending angle, set to 20° to best reproduce anisotropy spectra (see below), makes the S_2 state weakly 1PA-active and the S_1 state weakly 2PA-active; however, in both cases, the calculated

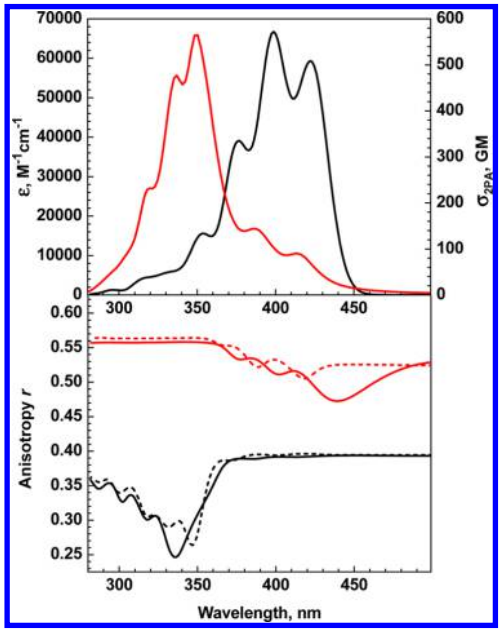

Figure 7. Top panel: Linear and 2PA spectra calculated for ε_{or} = 0.02 eV (to mimic the TOL solvent). Bottom panel: fluorescence anisotropy spectra calculated for ε_{or} = 0.07 eV (to mimic the pTHF solvent); continuous black and red lines refer to the results obtained in a liquid solvent upon one-photon and two-photon excitations, respectively. For comparison, dashed lines show anisotropies calculated in the hypothesis of a frozen solvent.

intensity of the nominally forbidden bands is small, which is in line with the experimental results. The μ_0 value in Table 2 was fixed to reproduce the 1PA intensity. With this choice, the value of the 2PA intensity is slightly overestimated.

The calculation of fluorescence anisotropy spectra accounting for vibrational coupling and for polar solvation is far from trivial. In refs 45 and 53−55, we addressed the calculation of one-photon-excited anisotropy spectra. Here, we extend the procedure to two-photon-excited spectra. The approach, rooted in the seminal work presented in refs 56−60, is described in detail in the Supporting Information. The results in Figure 7 are shown for ε_{or} = 0.07 eV to mimic the polarity of pTHF. This solvent is highly viscous, so we can safely assume that the solute molecules do not change their orientation during the excitation lifetime. However, pTHF is a liquid solvent, and it readjusts in response to the solute excitation, at variance with frozen solvents (glassy matrices), where the solvent is frozen in the ground-state configuration. For this specific case, results obtained for liquid and frozen solvents are similar (see Figure 7). The calculated linear and two-photon-induced anisotropies are in good agreement with the experiment, further confirming the reliability of the ESM approach. Even more importantly, we can now quantitatively discuss the origin of the anomalous behavior of the anisotropies when compared with the standard treatment. As discussed above, for the linear anisotropy, the standard model predicts r = 0.4 in the S_1 absorption region (fluorescence occurs from the same state) and r = −0.2 in the S_2 region (polarized perpendicularly to S1). For the two-photon-induced anisotropy, the standard model predictions are $r_{2PA} \approx 0.57$ in the S_2 region and $r_{2PA} \approx 0.14$ in the S_1 region. As discussed in the Supporting Information (see Figure S3), our calculation converges to this purely electronic result if we suppress the electron−vibration coupling (ε_v = 0) as well as the polar solvation (setting ε_{or} = 0). Thus, it is the concurrent effects of electron−vibration coupling and of polar solvation that, broadening the spectroscopic features, are responsible for the large observed deviation of the anisotropies from the results expected in a purely electronic model.

CONCLUSIONS

Comprehensive experimental and theoretical investigations of the linear photophysical and nonlinear optical properties of symmetrical fluorene derivative **1** were performed. The steady-state and time-resolved spectroscopic properties of **1** reveal an important fluorescence solvatochromism, suggesting symmetry breaking in the S_1 excited state. The degenerate 2PA spectrum of **1**, measured over a broad spectral range, shows the typical shape expected for centrosymmetric molecular structures with a maximum cross section of ∼200 GM. The values of two-photon excitation anisotropy are close to the theoretical maximum and exhibit a weak dependence on the excitation wavelength. The stimulated emission spectrum of **1** was obtained by a fluorescence quenching method, and a strong deviation of its maximum intensity from the corresponding maximum of the ground-state absorption cross section was shown. The nature of fast relaxation processes in **1** was revealed by femtosecond transient absorption spectroscopy, and potential for light amplification in a polar medium was noted as compared with that of well-known gain materials.

Experimental data were comprehensively analyzed based on an ESM that quantitatively describes linear and 2PA spectra of the dye in different solvents based on a handful of molecular parameters. We address not only the band positions and

DOI: 10.1021/acs.jpcc.7b12397
J. Phys. Chem. C XXXX, XXX, XXX−XXX

intensities, but, accounting for electron−vibration coupling and for polar solvation, we also address band shapes. This is particularly important for anisotropies where the spectral broadening due to the two interactions leads to large deviations from the results expected in the standard approach that only accounts for the mutual orientation of the electronic transition dipole moments. Our analysis demonstrates that in systems with sizable electron−vibration coupling and/or in the presence of inhomogeneous broadening due to polar solvation, a more accurate analysis of anisotropy data is needed to safely estimate the polarization direction. Similar important and nontrivial effects of electron−vibration coupling and polar solvation are demonstrated for two-photon-induced anisotropies, for which we present here the first explicit calculation of spectral band shapes. High fluorescence quantum yield, sizable 2PA cross section, potential light amplification, and acceptable photostability make **1** an interesting candidate for a number of nonlinear optical applications including STED microscopy.

■ ASSOCIATED CONTENT

Supporting Information

The Supporting Information is available free of charge on the ACS Publications website at DOI: 10.1021/acs.jpcc.7b12397.

Additional photophysical properties of **1**; ESM; detailed expressions for the calculation of linear and nonlinear optical spectra and two-photon-excited fluorescence anisotropies (PDF)

■ AUTHOR INFORMATION

Corresponding Authors

*E-mail: mbondar@mail.ucf.edu (M.V.B.).
*E-mail: anna.painelli@unipr.it (A.P.).

ORCID

Kevin D. Belfield: 0000-0002-7339-2813
Anna Painelli: 0000-0002-3500-3848

Notes

The authors declare no competing financial interest.

■ ACKNOWLEDGMENTS

This research was funded by the People Programme (Marie Curie Actions) of the European Union's Seventh Framework Programme FP7/2007-2013/ under REA grant agreement no. 607721 (Nano2Fun). M.V.B. acknowledges the support from the National Academy of Sciences of Ukraine (grants B-180 and VC/188). K.D.B. acknowledges the support from the National Science Foundation (CBET-1517273), while M.Y.C.G. acknowledges the support from the Arnold and Mabel Beckman Foundation and the University of Central Florida 2009 Beckman Scholars program. The authors thank Sheng Yao (University of Central Florida) for assistance in the synthesis of **1**. E.W.V.S. and D.J.H. thank the Army Research Laboratory (W911NF-15-2-0090) and the National Science Foundation grant DMR-1609895 for the support.

■ REFERENCES

(1) Cole, E. L.; Arunkumar, E.; Xiao, S.; Smith, B. A.; Smith, B. D. Water-Soluble, Deep-Red Fluorescent Squaraine Rotaxanes. *Org. Biomol. Chem.* **2012**, *10*, 5769−5773.

(2) Podgorski, K.; Terpetschnig, E.; Klochko, O. P.; Obukhova, O. M.; Haas, K. Ultra-Bright and -Stable Red and near-Infrared Squaraine Fluorophores for in Vivo Two-Photon Imaging. *PLoS One* **2012**, *7*, No. e51980.

(3) Yang, D.; Zhu, Y.; Jiao, Y.; Yang, L.; Yang, Q.; Luo, Q.; Pu, X.; Huang, Y.; Zhao, S.; Lu, Z. N,N-Diarylamino End-Capping as a New Strategy for Simultaneously Enhancing Open-Circuit Voltage, Short-Circuit Current Density and Fill Factor in Small Molecule Organic Solar Cells. *RSC Adv.* **2015**, *5*, 20724−20733.

(4) Bellani, S.; Iacchetti, A.; Porro, M.; Beverina, L.; Antognazza, M. R.; Natali, D. Charge Transport Characterization in a Squaraine-Based Photodetector by Means of Admittance Spectroscopy. *Org. Electron.* **2015**, *22*, 56−61.

(5) Webster, S.; Fu, J.; Padilha, L. A.; Przhonska, O. V.; Hagan, D. J.; Van Stryland, E. W.; Bondar, M. V.; Slominsky, Y. L.; Kachkovski, A. D. Comparison of Nonlinear Absorption in Three Similar Dyes: Polymethine, Squaraine and Tetraone. *Chem. Phys.* **2008**, *348*, 143−151.

(6) Belfield, K. D.; Bondar, M. V.; Haniff, H. S.; Mikhailov, I. A.; Luchita, G.; Przhonska, O. V. Superfluorescent Squaraine with Efficient Two-Photon Absorption and High Photostability. *ChemPhysChem* **2013**, *14*, 3532−3542.

(7) Avirah, R. R.; Jayaram, D. T.; Adarsh, N.; Ramaiah, D. Squaraine Dyes in PDT: From Basic Design to in Vivo Demonstration. *Org. Biomol. Chem.* **2012**, *10*, 911−920.

(8) Luo, C.; Zhou, Q.; Jiang, G.; He, L.; Zhang, B.; Wang, X. The Synthesis and $^1O_2$ Photosensitization of Halogenated Asymmetric Aniline-Based Squaraines. *New J. Chem.* **2011**, *35*, 1128−1132.

(9) Cumpston, B. H.; Ananthavel, S. P.; Barlow, S.; Dyer, D. L.; Ehrlich, J. E.; Erskine, L. L.; Heikal, A. A.; Kuebler, S. M.; Lee, I.-Y. S.; McCord-Maughon, D.; et al. Two-Photon Polymerization Initiators for Three-Dimensional Optical Data Storage and Microfabrication. *Nature* **1999**, *398*, 51−54.

(10) Kawata, S.; Kawata, Y. Three-Dimensional Optical Data Storage Using Photochromic Materials. *Chem. Rev.* **2000**, *100*, 1777−1788.

(11) Belfield, K. D.; Bondar, M. V.; Hernandez, F. E.; Przhonska, O. V.; Yao, S. Two-Photon Absorption Cross Section Determination for Fluorene Derivatives: Analysis of the Methodology and Elucidation of the Origin of the Absorption Processes. *J. Phys. Chem. B* **2007**, *111*, 12723−12729.

(12) Andrade, C. D.; Yanez, C. O.; Rodriguez, L.; Belfield, K. D. A Series of Fluorene-Based Two-Photon Absorbing Molecules: Synthesis, Linear and Nonlinear Characterization, and Bioimaging. *J. Org. Chem.* **2010**, *75*, 3975−3982.

(13) Yao, S.; Belfield, K. D. Two-Photon Fluorescent Probes for Bioimaging. *Eur. J. Org. Chem.* **2012**, 3199−3217.

(14) Belfield, K. D.; Bondar, M. V.; Morales, A. R.; Frazer, A.; Mikhailov, I. A.; Przhonska, O. V. Photophysical Properties and Ultrafast Excited-State Dynamics of a New Two-Photon Absorbing Thiopyranyl Probe. *J. Phys. Chem. C* **2013**, *117*, 11941−11952.

(15) Belfield, K. D.; Bondar, M. V.; Morales, A. R.; Padilha, L. A.; Przhonska, O. V.; Wang, X. Two-Photon STED Spectral Determination for a New V-Shaped Organic Fluorescent Probe with Efficient Two-Photon Absorption. *ChemPhysChem* **2011**, *12*, 2755−2762.

(16) Yue, X.; Armijo, Z.; King, K.; Bondar, M. V.; Morales, A. R.; Frazer, A.; Mikhailov, I. A.; Przhonska, O. V.; Belfield, K. D. Steady-State and Femtosecond Transient Absorption Spectroscopy of New Two-Photon Absorbing Fluorene-Containing Quinolizinium Cation Membrane Probes. *ACS Appl. Mater. Interfaces* **2015**, *7*, 2833−2846.

(17) Belfield, K. D.; Bondar, M. V.; Morales, A. R.; Yue, X.; Luchita, G.; Przhonska, O. V.; Kachkovsky, O. D. Two-Photon Absorption and Time-Resolved Stimulated Emission Depletion Spectroscopy of a New Fluorenyl Derivative. *ChemPhysChem* **2012**, *13*, 3481−3491.

(18) Githaiga, G. W.; Woodward, A. W.; Morales, A. R.; Bondar, M. V.; Belfield, K. D. Photophysical and Computational Analysis of a Symmetrical Fluorene-Based Janus Dione Derivative. *J. Phys. Chem. C* **2015**, *119*, 21053−21059.

(19) Belfield, K. D.; Bondar, M. V.; Morales, A. R.; Yue, X.; Luchita, G.; Przhonska, O. V. Transient Excited-State Absorption and Gain Spectroscopy of a Two-Photon Absorbing Probe with Efficient Superfluorescent Properties. *J. Phys. Chem. C* **2012**, *116*, 11261−11271.

DOI: 10.1021/acs.jpcc.7b12397
J. Phys. Chem. C XXXX, XXX, XXX−XXX

(20) Corredor, C. C.; Belfield, K. D.; Bondar, M. V.; Przhonska, O. V.; Yao, S. One- and Two-Photon Photochemical Stability of Linear and Branched Fluorene Derivatives. *J. Photochem. Photobiol., A* **2006**, *184*, 105−112.
(21) Wang, X.; Nguyen, D. M.; Yanez, C. O.; Rodriguez, L.; Ahn, H.-Y.; Bondar, M. V.; Belfield, K. D. High-Fidelity Hydrophilic Probe for Two-Photon Fluorescence Lysosomal Imaging. *J. Am. Chem. Soc.* **2010**, *132*, 12237−12239.
(22) Devi, C. L.; Yesudas, K.; Makarov, N. S.; Rao, V. J.; Bhanuprakash, K.; Perry, J. W. Fluorenylethynylpyrene Derivatives with Strong Two-Photon Absorption: Influence of Substituents on Optical Properties. *J. Mater. Chem. C* **2015**, *3*, 3730−3744.
(23) Xu, B.; He, J.; Liu, Y.; Xu, B.; Zhu, Q.; Xie, M.; Zheng, Z.; Chi, Z.; Tian, W.; Jin, C.; et al. High-Performance Two-Photon Absorption Luminophores: Large Action Cross Sections, Free from Fluorescence Quenching and Tunable Emission of Efficient Non-Doped Organic Light-Emitting Diodes. *J. Mater. Chem. C* **2014**, *2*, 3416−3428.
(24) Belfield, K. D.; Bondar, M. V.; Yao, S.; Mikhailov, I. A.; Polikanov, V. S.; Przhonska, O. V. Femtosecond Spectroscopy of Superfluorescent Fluorenyl Benzothiadiazoles with Large Two-Photon and Excited-State Absorption. *J. Phys. Chem. C* **2014**, *118*, 13790−13800.
(25) Yao, S.; Belfield, K. D. Synthesis of Two-Photon Absorbing Unsymmetrical Branched Chromophores through Direct Tris-(Bromomethylation) of Fluorene. *J. Org. Chem.* **2005**, *70*, 5126−5132.
(26) Lakowicz, J. R. *Principles of Fluorescence Spectroscopy*; Kluwer: New York, 1999.
(27) Magde, D.; Wong, R.; Seybold, P. G. Fluorescence Quantum Yields and Their Relation to Lifetimes of Rhodamine 6G and Fluorescein in Nine Solvents: Improved Absolute Standards for Quantum Yields. *Photochem. Photobiol.* **2002**, *75*, 327−334.
(28) Xu, C.; Webb, W. W. Measurement of Two-Photon Excitation Cross Sections of Molecular Fluorophores with Data from 690 to 1050 nm. *J. Opt. Soc. Am. B* **1996**, *13*, 481−491.
(29) Makarov, N. S.; Drobizhev, M.; Rebane, A. Two-Photon Absorption Standards in the 550-1600 nm Excitation Wavelength Range. *Opt. Express* **2008**, *16*, 4029−4047.
(30) Liu, T.; Bondar, M. V.; Belfield, K. D.; Anderson, D.; Masunov, A. E.; Hagan, D. J.; Van Stryland, E. W. Linear Photophysics and Femtosecond Nonlinear Spectroscopy of a Star-Shaped Squaraine Derivative with Efficient Two-Photon Absorption. *J. Phys. Chem. C* **2016**, *120*, 11099−11110.
(31) Fu, J.; Przhonska, O. V.; Padilha, L. A.; Hagan, D. J.; Van Stryland, E. W.; Belfield, K. D.; Bondar, M. V.; Slominsky, Y. L.; Kachkovski, A. D. Two-Photon Anisotropy: Analytical Description and Molecular Modeling for Symmetrical and Asymmetrical Organic Dyes. *Chem. Phys.* **2006**, *321*, 257−268.
(32) Belfield, K. D.; Bondar, M. V.; Hales, J. M.; Morales, A. R.; Przhonska, O. V.; Schafer, K. J. One- and Two-Photon Fluorescence Anisotropy of Selected Fluorene Derivatives. *J. Fluoresc.* **2005**, *15*, 3−11.
(33) Belfield, K. D.; Bondar, M. V.; Yanez, C. O.; Hernandez, F. E.; Przhonska, O. V. One- and Two-Photon Stimulated Emission Depletion of a Sulfonyl-Containing Fluorene Derivative. *J. Phys. Chem. B* **2009**, *113*, 7101−7106.
(34) Bashmakova, N. V.; Shaydyuk, Y. O.; Levchenko, S. M.; Masunov, A. E.; Przhonska, O. V.; Bricks, J. L.; Kachkovsky, O. D.; Slominsky, Y. L.; Piryatinski, Y. P.; Belfield, K. D.; Bondar, M. V. Design and Electronic Structure of New Styryl Dye Bases: Steady-State and Time-Resolved Spectroscopic Studies. *J. Phys. Chem. A* **2014**, *118*, 4502−4509.
(35) Shaydyuk, Y. O.; Levchenko, S. M.; Kurhuzenkau, S. A.; Anderson, D.; Masunov, A. E.; Kachkovsky, O. D.; Slominsky, Y. L.; Bricks, J. L.; Belfield, K. D.; Bondar, M. V. Linear Photophysics, Two-Photon Absorption and Femtosecond Transient Absorption Spectroscopy of Styryl Dye Bases. *J. Lumin.* **2017**, *183*, 360−367.
(36) Terenziani, F.; Painelli, A.; Katan, C.; Charlot, M.; Blanchard-Desce, M. Charge Instability in Quadrupolar Chromophores: Symmetry Breaking and Solvatochromism. *J. Am. Chem. Soc.* **2006**, *128*, 15742−15755.
(37) Boldrini, B.; Cavalli, E.; Painelli, A.; Terenziani, F. Polar Dyes in Solution:A Joint Experimental and Theoretical Study of Absorption and Emission Band Shapes. *J. Phys. Chem. A* **2002**, *106*, 6286−6294.
(38) Strickler, S. J.; Berg, R. A. Relationship between Absorption Intensity and Fluorescence Lifetime of Molecules. *J. Chem. Phys.* **1962**, *37*, 814−822.
(39) Birks, J. B.; Dyson, D. J. The Relations between the Fluorescence and Absorption Properties of Organic Molecules. *Proc. R. Soc. London, Ser. A* **1963**, *275*, 135−148.
(40) Azim, S. A.; Al-Hazmy, S. M.; Ebeid, E. M.; El-Daly, S. A. A New Coumarin Laser Dye 3-(Benzothiazol-2-yl)-7-Hydroxycoumarin. *Opt. Laser Technol.* **2005**, *37*, 245−249.
(41) El-Daly, S. A.; El-Azim, S. A.; Elmekawey, F. M.; Elbaradei, B. Y.; Shama, S. A.; Asiri, A. M. Photophysical Parameters, Excitation Energy Transfer, and Photoreactivity of 1,4-bis(5-Phenyl-2-Oxazolyl)-Benzene (POPOP) Laser Dye. *Int. J. Photoenergy* **2012**, *2012*, 458126.
(42) Hell, S. W.; Wichmann, J. Breaking the Diffraction Resolution Limit by Stimulated-Emission - Stimulated-Emission-Depletion Fluorescence Microscopy. *Opt. Lett.* **1994**, *19*, 780−782.
(43) Belfield, K. D.; Bondar, M. V.; Hernandez, F. E.; Przhonska, O. V.; Wang, X.; Yao, S. Superfluorescent Fluorenyl Probe with Efficient Two-Photon Absorption. *Phys. Chem. Chem. Phys.* **2011**, *13*, 4303−4310.
(44) Shafeekh, K. M.; Das, S.; Sissa, C.; Painelli, A. Asymmetric Squaraine Dyes: Spectroscopic and Theoretical Investigation. *J. Phys. Chem. B* **2013**, *117*, 8536−8546.
(45) Sissa, C.; Terenziani, F.; Painelli, A.; Siram, R. B. K.; Patil, S. Spectroscopic Characterization and Modeling of Quadrupolar Charge-Transfer Dyes with Bulky Substituents. *J. Phys. Chem. B* **2012**, *116*, 4959−4966.
(46) Terenziani, F.; Przhonska, O. V.; Webster, S.; Padilha, L. A.; Slominsky, Y. L.; Davydenko, I. G.; Gerasov, A. O.; Kovtun, Y. P.; Shandura, M. P.; Kachkovski, A. D.; Hagan, D. J.; Van Stryland, E. W.; Painelli, A. Essential-State Model for Polymethine Dyes: Symmetry Breaking and Optical Spectra. *J. Phys. Chem. Lett.* **2010**, *1*, 1800−1804.
(47) Campo, J.; Painelli, A.; Terenziani, F.; Regemorter, T. V.; Beljonne, D.; Goovaerts, E.; Wenseleers, W. First Hyperpolarizability Dispersion of the Octupolar Molecule Rystal Violet: Multiple Resonances and Vibrational and Solvation Effects. *J. Am. Chem. Soc.* **2010**, *132*, 16467.
(48) Hu, H.; Przhonska, O. V.; Terenziani, F.; Painelli, A.; Fishman, D.; Ensley, T. R.; Reichert, M.; Webster, S.; Bricks, J. L.; Kachkovski, A. D.; et al. Two-Photon Absorption Spectra of a Near-Infrared 2-Azaazulene Polymethine Dye: Solvation and Ground-State Symmetry Breaking. *Phys. Chem. Chem. Phys.* **2013**, *15*, 7666−7767.
(49) Kurhuzenkau, S. A.; Woodward, A. W.; Yao, S.; Belfield, K. D.; Shaydyuk, Y. O.; Sissa, C.; Bondar, M. V.; Painelli, A. Ultrafast Spectroscopy, Superluminescence and Theoretical Modeling of a Two-Photon Absorbing Fluorene Derivative. *Phys. Chem. Chem. Phys.* **2016**, *18*, 12839−12846.
(50) Terenziani, F.; D'Avino, G.; Painelli, A. Multichromophores for Nonlinear Optics: Designing the Material Properties by Electrostatic Interactions. *ChemPhysChem* **2007**, *8*, 2433−2444.
(51) Todescato, F.; Fortunati, I.; Carlotto, S.; Ferrante, C.; Grisanti, L.; Sissa, C.; Painelli, A.; Colombo, A.; Dragonetti, C.; Roberto, D. Dimers of Polar Chromophores in Solution: Role of Excitonic Interactions in One- and Two-Photon Absorption Properties. *Phys. Chem. Chem. Phys.* **2011**, *13*, 11099−11109.
(52) Sanyal, S.; Painelli, A.; Pati, S. K.; Terenziani, F.; Sissa, C. Aggregates of Quadrupolar Dyes for Two-Photon Absorption: The Role of Intermolecular Interactions. *Phys. Chem. Chem. Phys.* **2016**, *18*, 28198−28208.
(53) Sissa, C.; Painelli, A.; Blanchard-Desce, M.; Terenziani, F. Fluorescence Anisotropy Spectra Disclose the Role of Disorder in Optical Spectra of Branched Intramolecular-Charge-Transfer Molecules. *J. Phys. Chem. B* **2011**, *115*, 7009−7020.

DOI: 10.1021/acs.jpcc.7b12397
J. Phys. Chem. C XXXX, XXX, XXX−XXX

(54) Grisanti, L.; Terenziani, F.; Sissa, C.; Cavazzini, M.; Rizzo, F.; Orlandi, S.; Painelli, A. Polar Fluorenes and Spirobifluorenes: Fluorescence and Fluorescence Anisotropy Spectra. *J. Phys. Chem. B* **2011**, *115*, 11420−11430.
(55) Sissa, C.; Calabrese, V.; Cavazzini, M.; Grisanti, L.; Terenziani, F.; Quici, S.; Painelli, A. Tuning the Nature of the Fluorescent State: A Substituted Polycondensed Dye as a Case Study. *Chem.—Eur. J.* **2013**, *19*, 924−935.
(56) Monson, P. R.; McClain, W. M. Polarization Dependence of the Two-Photon Absorption of Tumbling Molecules with Application to Liquid 1-Chloronaphthalene and Benzene. *J. Chem. Phys.* **1970**, *53*, 29−37.
(57) McClain, W. M. Polarization Dependence of Three-Photon Phenomena for Randomly Oriented Molecules. *J. Chem. Phys.* **1972**, *57*, 2264−2272.
(58) McClain, W. M. Polarization of Two-Photon Excited Fluorescence. *J. Chem. Phys.* **1973**, *58*, 324−326.
(59) Callis, P. R. On the Theory of Two-Photon Induced Fluorescence Anisotropy with Application to Indoles. *J. Chem. Phys.* **1993**, *99*, 27−37.
(60) Callis, P. R. *Topics in Fluorescence Spectroscopy*; Lakowicz, J. R., Ed.; Plenum Press: New York, 1997; Vol. *5*, p 1.

DOI: 10.1021/acs.jpcc.7b12397
J. Phys. Chem. C XXXX, XXX, XXX−XXX